Energy-loss calculations for medium-energy rare gas $+H_2$ collisions

Ralph Snyder and Arnold Russek

Department of Physics, University of Connecticut, Storrs, Connecticut 06268

(Received 22 February 1982)

Cross sections differential in energy loss and scattering angle and most-probable reciprocal-mass functions are calculated for several rare gas on H_2 collisions in the low-keV collision-energy range. Specifically, the collision systems $He + H_2$, $Ne + H_2$, and $Ne^+ + H_2$ have been considered. The classical-trajectory calculations are based on a triatomic-molecular potential-functional form suggested by *ab initio* calculations of the He-H_2 energy surface, which serves as a prototype for all rare-gas-H_2 systems. The parameters in that functional form have been fitted from the experimental differential energy-loss measurements for Ne on H_2 collisions to yield the Ne-H_2 energy surface, and from the Ne^+ on H_2 differential energy-loss measurements to yield the Ne-H_2^+ energy surface. With the energy surfaces thus parametrized, the calculated differential energy-loss cross sections agree well with the experimental data. They explain the anomalously large range of scattering angle in which the collision is elastic, with no vibrational-rotational excitation.

I. INTRODUCTION

Recent energy-loss measurements in large-angle scattering experiments (up to 10 keV deg) of Ne^+ on H_2 and Ne on H_2 in the low-keV collision-energy range have suggested the existence of strong nonadditive valence forces deep in the repulsive region of the interaction energy surface,[1,2] a region previously thought to be dominated by vector additive forces generated by screened Coulomb core-core potentials. Until now, it has been supposed that valence forces are limited to relatively large separations. The experiments, however, demonstrated that these nonadditive valence forces extend deep into the repulsive region as well. In particular, Ne on H_2 collisions which lead to reduced scattering angles of 2 keV deg or less and Ne^+ on H_2 collisions which lead to reduced scattering angles of 5 keV deg or less seem to be almost completely elastic, despite the fact that the distance of closest approach between the Ne projectile and the H_2 target for 2 keV deg scattering is approximately equal to the H-H separation in the target, so that a large vibrational impulse had been expected. Moreover, a very significant difference was found between Ne on H_2 collisions and Ne^+ on H_2 collisions, indicating that core-core forces (which are almost unaffected by the difference between Ne and Ne^+) do not play a dominant role in these collisions.

These surprising results motivated an *ab initio* study of the simpler He-H_2 energy surface in the repulsive region to serve as a prototype for all rare-gas-H_2 collision systems,[3] inasmuch as He^+ on H_2 collisions[4] behave in a manner quite similar to Ne^+ on H_2 collisions. The *ab initio* calculations did indeed bear out the experimental conclusions of Refs. 1 and 2. The He-H_2 calculated energy surface is rather well fit by the parametric form[3]:

$$V(R,r,\gamma) = Z_p \left[\frac{e^{-\lambda_c R_A}}{R_A} + \frac{e^{-\lambda_c R_B}}{R_B} \right]$$
$$+ A_2(e^{-\lambda_p R_A} + e^{-\lambda_p R_B})$$
$$+ A_3 e^{-\lambda_p R} - Be^{-bR}, \qquad (1)$$

which should also be valid for all rare-gas-H_2 systems as well. Here, Z_p is the nuclear charge of the projectile, A_2 is the strength of the two-body polarization potential, and A_3 gives the strength of the long-range part of the three-body polarization potential, the term that gives rise to the nonadditive forces. The term Be^{-bR} is a short-range contribution which describes the saturation of the three-body term in the vicinity of $R=0$. The geometry is described in the preceding paper,[3] which also gives, in Table II, the values of the parameters yielding the best fit to the *ab initio* calculations of the He-H_2 system. The three-body term is a function only of R, the distance between the projectile and the *center*

of the H_2 target. It can, therefore, contribute only to elastic scattering; it cannot contribute to rotational or vibrational excitation. It arises from the fact that the electrons in an H_2 molecule are somewhat drawn into the region between the two protons, at the expense of the distributions centered about each proton; it is this distribution, centered at $R = 0$, that causes the three-body potential. The polarization potentials are repulsive, due to the Pauli exclusion principle which forbids the overlap of electrons in *phase space*. Thus, the spatial overlap of the He and H_2 distributions at small separations causes an increase in the momentum distribution and, therefore, in the electronic energy. Characteristically, the Born—Mayer-type polarization terms are long range, while the core-core Bohr terms are short range. The two-body polarization term has a small amplitude and is, moreover, only weakly able to cause vibrational or rotational excitation. Thus, larger impact parameter collisions will be almost completely elastic. However, a Born-Mayer potential has a maximum value of τ that it is able to produce, whereas the core-core Bohr potential can produce all center-of-mass (c.m.) scattering angles up to 180°. Thus, the potential given by Eq. (1) will give rise to essentially elastic scattering for scattering angles with τ below some critical value, the maximum that can be produced by the polarization term. Beyond that critical value of τ, the core-core terms must contribute, and with that contribution will come vibrational-rotational excitation.

In this paper, the dependence of the energy loss on τ is quantified, detailed calculations for He-H_2, Ne-H_2, and Ne$^+$-H_2 collisions are presented. The results for Ne + H_2 and Ne$^+$-H_2 collisions are in good agreement with existing experimental results.

II. THEORY

It is by now becoming standard to discuss energy loss in atom-molecule collisions in terms of a reciprocal mass function, f. This parameter is obtained by analogy with simple potential scattering of a projectile of mass M_P by a target of mass M_T, where kinematics alone determines that the projectile energy loss T, the projectile energy E, and the scattering angle θ are related by $M_P/M_T = T/E\theta^2$. For collisions of helium projectiles with H_2 targets which occur without electronic excitation (but in which vibrational-rotational excitation may occur), one can still define an effective molecular mass, M_{eff}, by the equation

$$M_P/M_{\text{eff}} = T/E\theta^2 . \tag{2}$$

For gentle collisions with impact parameters much larger than the H-H separation in the target molecule, M_{eff} will be very nearly the entire molecular mass, $2M_H$. On the other hand, for hard collisions, the high momentum transfer involved can be achieved only if the distance of closest approach between the projectile and one of the target nuclei is much less than the H-H separation in the H_2. In this latter case, M_{eff} will be very nearly equal to M_H, since the other H remains behind as a distant spectator. This suggests, and several experiments confirm,[1,2,4-6] that the dimensionless reciprocal mass function f, introduced by Sigmund[7] and defined by

$$f = M_H/M_{\text{eff}} , \tag{3}$$

takes on values between 0.5 (the elastic limit) and 1.0 (the binary limit). The function f is, then, a scaled energy loss, a convenient parameter which determines how inelastic a given atom-molecule collision is. Its use does not entail the loss of any information, inasmuch as both the projectile energy loss, T, and vibrational-rotational inelastic energy, Q, are determined by f and the scattering angle. The inelastic energy is just the difference between the total energy lost by the projectile and the translational recoil energy of the target mass $M_T = 2M_H$:

$$Q = T - P^2/2M_T , \tag{4}$$

where, for small scattering angle, the collisional momentum transfer P is the incident momentum multiplied by the scattering angle,

$$P = (2M_P E)^{1/2}\theta . \tag{5}$$

From the definitions (2) and (3),

$$f = M_H/M_{\text{eff}} = M_H T/M_P E\theta^2$$
$$= \tfrac{1}{2} T/(P^2/2M_T) , \tag{6}$$

and from Eqs. (4)—(6), T and Q are given by

$$T = 2fE\theta^2 M_P/M_T , \tag{7}$$

$$Q = (2f - 1)E\theta^2 M_P/M_T . \tag{8}$$

Sigmund[7,8] first suggested that, under rather general conditions which are expected to be valid in the keV collision energy regime, f will depend only on the reduced scattering angle $\tau = E\theta$. These conditions are (i) classical scattering and (ii) the sudden approximation for the motion of the nuclei (electronic motion continues to be treated adiabatically).

Reference 7 also contained a third condition requiring the collision forces between projectile and target molecule to be vector-additive binary forces. With the indication from the present work and Ref. 3 that the scaling law seemed to be valid even without binary forces, Sigmund[8] generalized the original derivation to arbitrary forces derivable from a potential. Sigmund scaling thus requires only the two assumptions listed above and will be valid for nonadditive polarization forces as well as binary forces.

Following Sigmund, Fig. 1 shows the geometry of a collision projected onto the target plane, a plane perpendicular to the projectile velocity which contains the center of mass of the target molecule. Thus, the projected H-H separation, d, of Fig. 1 is $r\sin\alpha$, where $\vec{r}$ is the full H-H separation and α is the angle between $\vec{r}$ and the projectile velocity. This work presents results for equilibrium H-H separation, $1.4a_0$. Additional calculations were also made in the range $1.2 \leq r \leq 1.6a_0$ and show that calculations at equilibrium r give the same results as is obtained by averaging over ground-state vibrational separations. The target plane contains the impact parameters $\vec{b}_1$ and $\vec{b}_2$ of the helium projectile with respect to the near and far hydrogen atoms, and $\vec{b}_3$, the impact parameter with respect to the *center* of the target molecule. The $\vec{b}_i$ are written as vectors in the target plane, because the directions as well as the magnitudes are important. These $\vec{b}_i$ determine the reduced scattering angles $\vec{\tau}_i$, with $\vec{\tau}_1$ and $\vec{\tau}_2$ being determined by the binary forces, while $\vec{\tau}_3$ is determined by the three-body polarization force. The impact expansions[9] of the reduced scattering angles are useful here:

$$V(\rho) = (V_0/\rho)\exp(-c\rho) ,$$
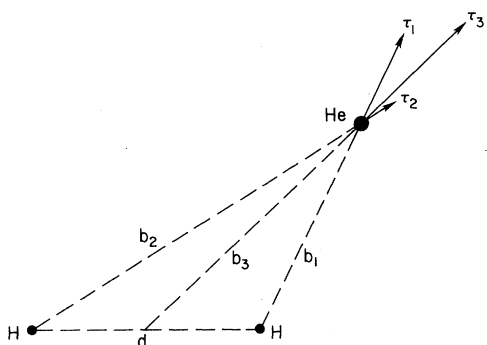
$$\tau = cV_0 K_1(cb) + O(E^{-1}) \tag{9}$$

FIG. 1. He + H_2 collision geometry projected onto the target plane. b_i are impact parameters and τ_i are reduced scattering angles, $E\theta_i$.

and

$$V(\rho) = V_0\exp(-c\rho) , \tag{10}$$

$$\tau = cbV_0 K_0(cb) + O(E^{-1}) ,$$

where ρ stands for R_A, R_B, or R and where K_0 and K_1 are the modified Bessel functions. Bernstein[10] has derived the leading term in Eq. (10) from a quantal phase-shift argument. For the small scattering angles considered in this work, the terms proportional to E^{-1} are negligible, a fact which plays an important role in securing the scaling property described by Sigmund. In order to minimize the confusion which can arise from conflicting jargons, it may be noted that the scattering angles considered in this work range up to a few degrees in the laboratory frame. These are termed "large angle scattering" in the experimental jargon, yet are well within the "small angle scattering" range of the theorists' jargon. In this small scattering angle approximation, impulses parallel to the projectile velocity are negligible, so that the reduced scattering angles $\vec{\tau}_1$, $\vec{\tau}_2$, and $\vec{\tau}_3$ all lie in the target plane and add vectorially to yield the net scattering angle, $\vec{\tau}$:

$$\vec{\tau} = \vec{\tau}_1 + \vec{\tau}_2 + \vec{\tau}_3 . \tag{11}$$

The energy lost by the projectile is the sum of the energies acquired by the two H atoms in the target molecule:

$$T = T_1 + T_2 = P_1^2/2M_H + P_2^2/2M_H , \tag{12}$$

where $\vec{P}_1$ and $\vec{P}_2$ are the separate recoil momenta of each H. Because the force giving rise to $\vec{\tau}_3$ is exerted against the H_2 center of mass, it is equally divided between both H atoms. Thus,

$$\vec{P}_1 = (2M_P/E)^{1/2}(\vec{\tau}_1 + \tfrac{1}{2}\vec{\tau}_3) , \tag{13a}$$

$$\vec{P}_2 = (2M_P/E)^{1/2}(\vec{\tau}_2 + \tfrac{1}{2}\vec{\tau}_3) , \tag{13b}$$

and

$$T = (M_P/M_H E)$$
$$\times [\tau_1^2 + \tau_2^2 + \tfrac{1}{2}\tau_3^2 + \vec{\tau}_3 \cdot (\vec{\tau}_1 + \vec{\tau}_2)] . \tag{14}$$

Substitution of (14) into (6) yields

$$f = \tau^{-2}[\tau_1^2 + \tau_2^2 + \tfrac{1}{2}\tau_3^2 + \vec{\tau}_3 \cdot (\vec{\tau}_1 + \vec{\tau}_2)] , \tag{15}$$

where $E\theta$ has been replaced by τ.

From Eqs. (1), (9), (10), and (15), it is clear that f, so calculated, is a function of impact parameters only. It is, therefore, independent of E or θ separately, and will be a universal function of

$\tau = E\theta$. This is a specific realization of Sigmund's scaling principle.

The above equations define the outcome of a single projectile-target collision at a given impact configuration defined by impact parameters b_i and the orientation angle α of the molecular target. In order to determine cross sections, τ and f were thus calculated from Eqs. (11) and (15) and stored for, typically, 10^5 different impact configurations, sampling sufficient values of both impact positions and molecular orientation angle to secure good numerical convergence. The number of configurations which result in scattering into reduced scattering angles between τ and $\tau + \Delta\tau$ with a scaled energy loss between f and $f + \Delta f$ then determine the doubly differential cross sections.

III. RESULTS

The most-probable scaled energy losses, f_m, are shown plotted as functions of τ in Fig. 2. These plots have been the feature of central concern in the recent literature. The curve marked A in this figure presents the scaled most-probable energy losses for He on H_2 or He on D_2 collisions obtained with the *ab initio* calculated He-H_2 interaction potential, the parameters for Eq. (1) being taken from Table II of Ref. 3. It will be noted that Eq. (15) predicts identi-

cal values of f_m for H_2 and D_2 targets. At present, no experimental data for this collision system are available for direct comparison with the theoretical results, but the qualitative features for this system are expected to be similar to the energy losses both in Ne on D_2 and Ne$^+$ on D_2 scattering, both of which have been measured. For want of other experimental data, it is these neon on molecular deuterium experimental results which are compared here with the theory. Suitable parameters for the Ne-D_2 and (Ne-D_2)$^+$ potentials are easily determined by fitting the scattering data. Of course, $Z_P = 10$, and λ_c is taken to be proportional to $(1 + Z_P^{2/3})^{1/2}$, as suggested by Thomas-Fermi arguments [cf. Eq. (17b) below] so that for, neon projectiles, the exponential parameter λ_c, scaled from the value for helium projectiles, is $\lambda_c = 4.72a_0^{-1}$. It is shown analytically below that the dependence of f_m on τ is relatively insensitive to the details of the core-core potentials, but quite sensitive to the three-body potentials and, in particular, to the maximum scattering angles which they produce. These are largely determined by the strength parameters A_3 and B, which have therefore been determined by optimizing the agreement in Fig. 2. The resulting values for the Ne-D_2 system are $A_3 = 6$, $B = 4.75$; for the (Ne-D_2)$^+$ system, $A_3 = 20$ and $B = 15.8$. All other parameters have been kept the same as for the He-H_2 system, for lack of any calculated values for
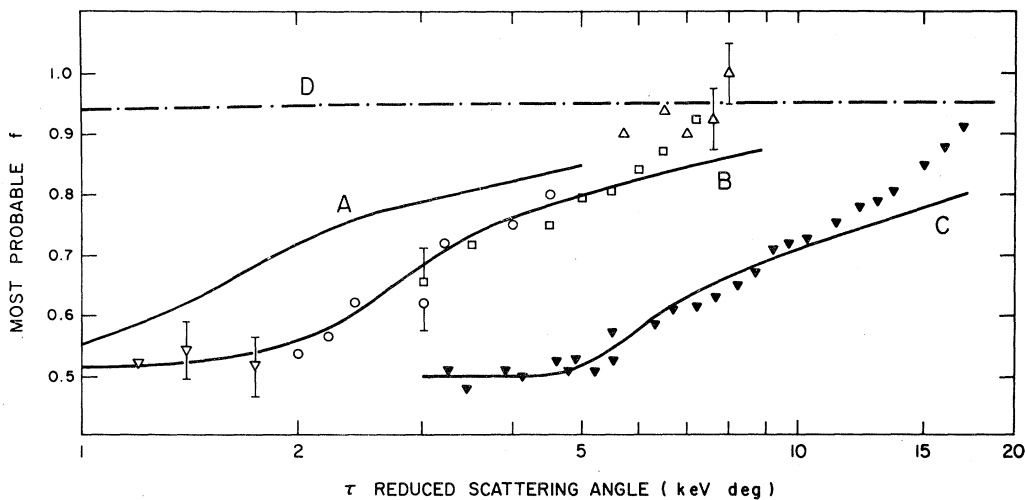

FIG. 2. Most-probable scaled energy loss of the projectile plotted as a function of reduced scattering angle. Curve A shows the calculated results obtained using the *ab initio* potential for the He-H_2 system. Curves B and C show the Ne $+ D_2$ and Ne$^+ + D_2$ calculations using potentials of the form Eq. (1) with parameters empirically fitted for each collision system. Calculations are described in Sec. II. Experimental points from Ref. 2 are also shown. Open points give the results for Ne on D_2 corresponding to projectile energies of 0.5 keV, $\triangledown$; 1.0 keV, $\bigcirc$; 1.5 keV, $\square$; and 2.0 keV, $\triangle$. Results for Ne$^+ + D_2$ collisions at projectile energy 3.5 keV are represented by a solid nablus. Curve D shows the results obtained for Ne or Ne$^+$ on D_2 using the Bohr two-center potential given by Eq. (17).

the Ne-H$_2$ or (Ne-H$_2$)$^+$ systems. The details of the core-core potentials are not important in an f_m vs τ plot, but uncertainty in the value of λ_p, which gives the range of polarization forces, may be a serious defect. Ultimately, both A_3 and λ_p can be experimentally determined by carefully measuring the differential scattering cross section in the completely elastic angular region below the critical value of τ and inverting these measurements to yield the long-range tail of the scattering potential; thus far, however, no such measurements have been made.

Curve B in Fig. 2 shows the calculated value of f_m vs τ for Ne on D$_2$ (or H$_2$) collision, while curve C shows the results for Ne$^+$ on D$_2$ (or H$_2$) collisions. In the range of $\tau \leq 2$ keV deg for Ne on D$_2$ collisions, a detailed analysis shows that the statistically predominant collisions are those close to the midplane of the molecular target, $b_1 \approx b_2$. For values of τ larger than 2 keV deg, f_m rises above 0.5 and asymptotically approaches the binary limit of 1.0. The three-body forces alone cannot produce such large values of τ, and the core-core forces necessarily play an important, and asymptotically dominant, role in the scattering. Moreover, the calculations for Ne on D$_2$ show that, for $\tau \geq 4$ keV deg, the statistically dominant region of Fig. 1 is the projected internuclear axis, so that $b_2 \approx d + b_1$. In this region, an explicit formula for the dependence of f upon τ can be easily obtained from Eq. (15) by making the mild approximation that the effect of the distant target atom is negligible compared to either the near target atom or the three-body force, so that $\tau_2 \ll \tau_1$ or τ_3. One easily finds that

$$f = 1 - \tau_3/\tau + \tfrac{1}{2}\tau_3^2/\tau^2 . \tag{16}$$

Furthermore, τ_3 is very nearly a constant for large τ, because for all impact parameters in the range

$$0.4a_0 \leq b_3 \leq 0.9a_0 ,$$

τ_3 is within 10% of its maximum value, 1.2 keV deg for Ne-H$_2$. Since a large value of τ can only result from a close collision with one target atom, b_3 usually falls within that rather broad range, and it is possible to set $\tau_3 = 1.2$ keV deg. Equation (16) is then a quadratic in $1/\tau$, which approximates the calculated results of curve B very well not only at large τ, where the above arguments apply, but, surprisingly, for all values of τ beyond 1.2 keV deg. Similarly, if for Ne$^+$ on D$_2$ scattering the value of τ_3 is set equal to 4 keV deg, (the maximum value of τ_3), then Eq. (16) agrees quite well with curve C for all τ beyond 4 keV deg. Remarkably, Eq. (16) does not depend on the detailed form of the core-core in-

teractions, except that they be short range and strong enough to produce large τ, nor does it depend sensitively on the projected internuclear separation d. The maximum value of τ_3 emerges as a dominant feature, which determines the parameters of the three-body terms in the potential. Along with the results calculated in this work, Fig. 2 also shows the experimental data points from Andersen et al.[2] for collisions involving Ne and Ne$^+$ projectiles with D$_2$. The theory agrees closely with experiment except at large values of τ, where spurious counts arising from electronic excitation may have artificially raised the f values.[11] The difference, for example, between the experimental and calculated values for Ne on D$_2$ at $\tau = 8$ keV deg, corresponds to an excess energy loss of 14 eV, which is comparable to electronic excitation energies of the projectile and the target.

The threshold behavior of f_m as it first begins to rise above the elastic limit, 0.5, is an interesting aspect of the energy-loss dynamics which should be studied in higher resolution in future work. Equation (16) predicts the rise to be parabolic, with $f_m - \tfrac{1}{2}$ proportional to $(\tau - \tau_3^{\max})^2$ near $\tau_3^{\max}$. The currently available experimental data shown in Fig. 2 lend some support to such a parabolic rise, but since (16) is, in principle, a high τ approximation with no a priori claim to validity near the elastic limit, further study is required.

Finally, curve D in Fig. 2 shows for comparison the single curve representing both Ne on D$_2$ and Ne$^+$ on D$_2$ predicted by a strict vectorially additive two-body Bohr potential:

$$V = Z_p/R_A \exp(-\lambda_c R_A) + Z_p/R_B \exp(-\lambda_c R_B) , \tag{17a}$$

$$\lambda_c = (1 + Z_p^{2/3})^{1/2} . \tag{17b}$$

Here, Z_p is again the projectile charge and Z, for each target atom, has been set equal to unity. The resulting f_m hovers very close to unity over the entire range of reduced scattering angle here considered. This is because the effects of the two-center Bohr potential fall off rapidly with distance, so that even in distant $(b \gg d, \lambda_c^{-1})$ encounters resulting in small scattering angles, the ratio τ_2/τ_1 can be very small, of order $e^{-\lambda_c d}$. The reciprocal mass function is then approximately given by

$$\cosh\lambda_c d /(1 + \cosh\lambda_c d) ,$$

which is nearly unity for Ne$^{0,+}$ + D$_2$ collisions. Thus, with the potential of Eq. (17) even distant

collisions end up near the binary limit, whereas potentials of the form of Eq. (1) avoid this unrealistic feature, since they contain the important three-body polarization forces, as discussed above.

Figure 3 shows the calculated doubly differential energy cross sections for the Ne^+ on D_2 (or H_2) collision system. It is seen that the energy-loss dependence of the calculated cross section obtained with the parametrically fitted potential of the form given by Eq. (1) is a rather sharply peaked function. Indeed, it is for this reason that there is a most-probable energy loss, f_m, associated with each reduced scattering angle τ. Information is contained in the width and shape of the peak which, if experimentally determined, can yield valuable information on the range of the core-core part of the triatomic-molecular potential. In the vicinity of the critical value of τ, at which the crossover occurs from dominant scattering by the three-body forces to dominant scattering by the core-core forces, if the range of the core-core potential is not much smaller than the three-body valence potential, the line shape of the energy-loss cross section becomes broad and can even exhibit a doubly peaked structure. This behavior is illustrated in Fig. 4 for a vectorially additive two-body Bohr potential. Such a potential has no three-body part; hence, the anomalously broad line is found at small values of τ. For the potential of the form Eq. (1) used to generate curve C for Ne^+ on D_2 collisions, the anomalously broad line shape would occur at $\tau \simeq 6$ keV deg, were the range of the core-core potential significantly longer
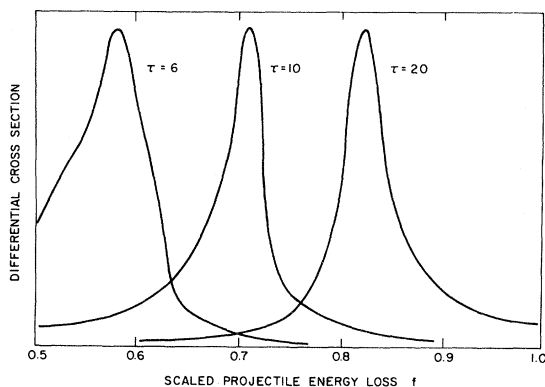
than that used for curve C.

No such doubly peaked line shape has been seen in the experimental data.[2] Unfortunately, experimental resolution problems do not yet allow any firm conclusions to be drawn. It is not difficult to demonstrate that most, if not all, of the experimental linewidths are due to experimental resolution. Taking the differential of T as given by Eq. (7), considering f, E, and θ all to be variables,

$$\delta T = (2M_p/M_T)$$
$$\times (E\theta^2\delta f + E\theta^2 f\delta E/E + 2fE\theta\delta\theta) .$$

$$(18)$$

For Ne or Ne^+ on D_2, with the energy loss T measured in eV while the beam energy E is measured in keV and θ in deg,

$$\delta T = 3.1E\theta^2\delta f + 3.1E\theta^2 f\delta E/E + 6.1fE\theta\delta\theta .$$

$$(19)$$

The first term of (17) is the natural linewidth, due to the fact that collisions which result in a given scattering angle τ can give rise to a range of values for T. The second and third terms describe contributions to the linewidth δT due to beam energy and angular widths. Since

$$\delta E/E = 0.0005$$

for the experiment, this term is negligible. On the other hand, using the value 0.25° quoted by Andersen et al.[2] for the angular width of the beam, over 60% of the widths for δT shown in their Fig. 1 is

FIG. 3. Doubly differential cross sections for Ne^+ on D_2 collisions plotted as functions of scaled energy loss, f, at $\tau = 6$, 10, and 20 keV deg. Calculations were carried out as described in Sec. II, through the use of a potential of the form Eq. (1) with the parameters empirically fitted for the $(Ne-D_2)^+$ system. Respective maxima in the doubly differential cross section are located at 1.2, 0.27, and $0.062a_0^2/keV$ deg.
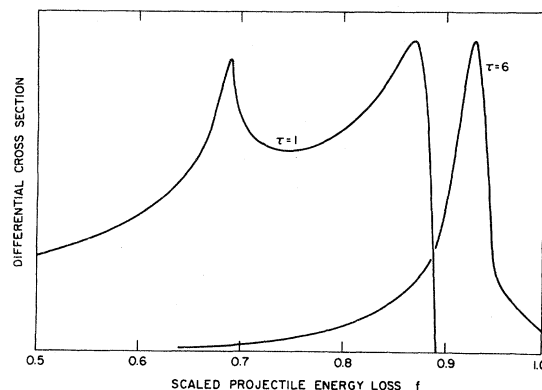

FIG. 4. Doubly differential cross sections calculated with a binary Bohr potential, Eq. (17). Broad double peak seen at small values of τ arises from the fact that small scattering angles can be produced by either large impact parameter collisions, which produce small f, or collisions in which the projectile goes through the center of the target molecule, which produce large f.

due to this cause. Moreover, these linewidths are found to vary directly with $E\theta$, and not $E\theta^2$, suggesting that all, or nearly all, of their linewidths are due to angular resolution, with an uncertain contribution from the natural linewidth δf. Even so, a really broad line of the form seen in Fig. 4 should show up in the experimental linewidths if it existed. In any event, it will be extremely interesting to examine future experimental work on the line shapes carried out with higher angular resolution.

[1]N. Andersen, M. Vedder, A. Russek, and E. Pollack, J. Phys. B 11, 1493 (1978).

[2]N. Andersen, M. Vedder, A. Russek, and E. Pollack, Phys. Rev. A 21, 782 (1980).

[3]A. Russek and R. Garcia G., Phys. Rev. A 26, 1924 (1982), paper I.

[4]A. V. Bray, D. S. Newman, and E. Pollack, Phys. Rev. A 15, 2261 (1977).

[5]J. Fayeton, A. Pernot, P. Fournier, and M. Barat, J. Phys. (Paris) 32, 743 (1971).

[6]S. M. Fernandez. F. J. Eriksen, A. V. Bray, and E. Pollack, Phys. Rev. A 12, 1252 (1975).

[7]P. Sigmund, J. Phys. B 11, L145 (1978).

[8]P. Sigmund, J. Phys. B 14, L321 (1981).

[9]C. Lehmann and G. Leibfried, Z. Phys. 172, 465 (1963); see also F. T. Smith, R. P. Marchi, and K. G. Dedrick, Phys. Rev. 150, 79 (1966).

[10]R. B. Bernstein, J. Chem. Phys. 38, 515 (1963).

[11]E. Pollack, private communication.